Characterizing the Role of Homeostatic Plasticity in Central Pattern Generators

Lindsay Stolting, Randall D. Beer and Eduardo J. Izquierdo

Cognitive Science Program and Program in Neuroscience, Indiana University Bloomington
lstoltin@iu.edu

Abstract

Various models have been developed to shed light on neuronal mechanisms of homeostatic plasticity (HP). We focus on one such model implemented on continuous-time recurrent neural networks. Though this HP mechanism encourages oscillatory dynamics by preventing node saturation, it was curiously detrimental to behavioral fitness when compared to non-plastic networks on several tasks (Williams, 2004, 2005). When we set out to explain this result, we discovered a type of oscillation that *depends on* HP's continued regulation of circuit parameters. If HP is turned off, oscillation stops. This suggests that HP can play an enabling role in central pattern generation which has not been explored in modelling or experimental contexts. We first situate this phenomenon within the space of possibilities for HP's involvement in oscillation. Then, we show that these "HP-enabled" oscillations are extraordinarily common in random circuits of various sizes. Finally, we describe how the degree of timescale separation between HP and neural dynamics affects HP-enabled oscillation. This analysis suggests promising avenues for dialogue between modeling and experiment.

Introduction

It is known that neurons in many organisms tune both their excitability and synaptic sensitivity to counteract prolonged periods of over- or under-excitation (Turrigiano et al., 1994; Davis, 2006; Turrigiano, 2012). Collectively, these processes are dubbed activity-dependent homeostatic plasticity (HP). A myriad of cellular mechanisms for such homeostatic plasticity have been proposed and empirically supported to date, ranging from neuron-wide tuning of channel densities, to synapse-specific regulation of receptor concentration, quantal amplitude scaling, and spike-time-dependent plasticity (Watt and Desai, 2010; Olypher and Prinz, 2010; O'Leary et al., 2014; Turrigiano and Nelson, 2004; Northcutt and Schulz, 2019). These mechanisms act on multiple different timescales, as demonstrated by results from various experimental paradigms examining the response of HP to acute perturbations (Schulz and Lane, 2017). Following the removal of afferents, blockage of K^+ channels, or K^+ inundation, circuit activity levels can recover within days, hours, or even minutes, respectively (Lane et al., 2016; Thoby-Brisson and Simmers, 2000; He et al., 2020).

Various biophysical models have been formulated to test what may result from a given set of homeostatic cellular mechanisms. For example, Olypher and Prinz (2010) modeled activity-dependent homeostatic regulation of conductance densities in a Morris-Lecar neuron and proposed a mechanism for the recovery of dynamics after loss of neuromodulation in the stomatogastric ganglion. Moreover, Abbott and LeMasson (1993) and Günay and Prinz (2010) demonstrated how a model calcium sensor could affect downstream targets to confer network stability. Models have even been able to suggest that activity sensors on multiple timescales may be necessary for HP to maintain more complex patterns of activity, like bursting (Liu et al., 1998). In general, the idea is that HP configures neural parameters in such a way that the circuit behaves, and maintains this configuration.

Several researchers have implemented computationally simpler models of HP in behaving networks, in order to assess its role in brain-body-environment systems. One family of such models realizes activity dependent HP in continuous-time recurrent neural networks (CTRNNs). For example, Di Paolo (2000, 2002) applied changes to the bias of each node throughout the duration of a phototaxis task to ensure that the average activity approached a central value of 0.5 in the long term. It was observed that these homeostatic networks were more robust to perturbations such as sensor lesions and inversion not seen during the course of their evolution.

Taking inspiration from Di Paolo's original formulation, Williams (2004) proposed an activity-dependent HP mechanism which prevents saturation of CTRNN nodes by dynamically adjusting their incoming synaptic weights and intrinsic biases in the direction most likely to restore output levels within a given target range. After utilizing this mechanism for a time, randomly initialized circuits were, of course, more likely to oscillate and showed better signal propagation because they had been pushed towards the center crossing region of parameter space (Di Paolo, 2000; Williams, 2006; Williams and Noble, 2007; Mathayomchan and Beer, 2002). Additionally, such homeostatic circuits could per-

form phototaxis, shape discrimination, and ball-catching, and were more robust to sensor inversion and random noise in these paradigms (Williams, 2004, 2005). Curiously however, homeostatic agents performing all three of these tasks were reported to be somewhat less evolvable and less fit than their static counterparts. As such, it was suggested that the problem must be with allowing HP mechanisms to remain active concurrently with the performance of behavior, and that HP might be more useful during a kind of developmental period, after which point it is switched off. Resigning to this, however, would greatly reduce the attractiveness of HP as a method of conferring robustness to artificial networks; what about perturbations experienced after this critical period? Moreover, the analogy to biology would be lost since neuronal homeostatic plasticity responds to perturbation within otherwise normally behaving circuits. Clearly, more needs to be understood about the role of HP acting concurrently during behavior and why it may have led to behavioral disruption.

In order to investigate this question, we will implement the HP mechanism proposed by Williams (2004) in CTRNNs performing a tractably simple but non-trivial task: oscillation at a target frequency. After overviewing the network model, we begin by evolving successful three-neuron circuits. Curiously, we find that in some of these networks, turning HP "off" (freezing weight and bias values) stops oscillations. Upon second inspection, this makes sense because the implementation of HP turns these neural "parameters" into changing states of the system, thereby increasing its dimensionality. Certain kinds of limit cycles are realized only in the full homeostatic system and are thus not captured by analyses which approximate weights and biases as constant. We call these oscillations in which HP plays a constitutive role "HP-enabled" and contrast them with oscillations which were induced by HP but do not continually require it.

To explain this phenomenon, we implement a stripped-down version of the model, wherein we characterize the role of HP in three qualitatively different scenarios. Returning to the full system, we examine whether HP is more likely to play an enabling and continually active role in oscillation or to simply induce it. Then, we will ask how the degree of timescale separation between the rate of change of the neural states and the action of HP affects HP's influence on oscillatory frequency. Finally, we summarize the work and discuss opportunities for future study.

Methods

Our base network model is a continuous-time recurrent neural network (CTRNN). CTRNNs have been widely used as a behavioral and evolutionary substrate for a variety of tasks because their dynamics are rich and nonlinear. They are defined by a set of equations governing the rate of change of the state of each node, which take the form:

$$\tau_i \dot{y_i} = -y_i + \sum_{j=1}^{N} w_{ji}\sigma(y_j + \theta_j) \tag{1}$$

where y_i represents the state of node i, τ_i is its time-constant, θ_i is its bias, and w_{ji} is the synaptic weight connecting unit j to unit i. The output of neuron i (o_i) is defined as $\sigma(y_i + \theta_i)$ where σ is the sigmoid function $\sigma(x) = 1/1 + e^{-x}$.

The homeostatic plasticity mechanism we employ was originally formulated by Williams (2004). When the activity level of any neuron falls outside a central target range, the mechanism activates and adjusts the incoming weights (w_{ji}) and bias values (θ_i) in the direction necessary to restore it. These changes are governed by the following differential equations,

$$\tau_w \dot{w_{ji}} = \rho_i |w_{ji}| \tag{2}$$

$$\tau_\theta \dot{\theta_i} = \rho_i \tag{3}$$

where τ_w determines the rate of plasticity for the weights, τ_θ the rate of plasticity for the biases, and the plastic facilitation parameter ρ_i is calculated as a function of the neuron outputs (o_i) according to

$$\rho_i = \begin{cases} \frac{LB - o_i}{LB} & : 0 < o_i < LB \\ 0 & : LB \leq o_i \leq UB \\ \frac{UB - o_i}{1 - UB} & : UB < o_i < 1 \end{cases} \tag{4}$$

.

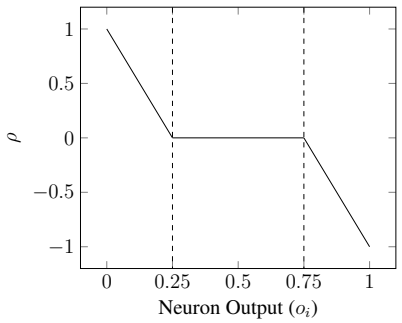

For consistency with Williams (2005), the upper and lower bounds of the target range will be set to 0.25 and 0.75 and the time constants for the homeostatic equations will be set to $\tau_w = 40$ and $\tau_\theta = 20$, unless otherwise specified. All code and data can be accessed at https://github.com/ljstolting/RoleofHPinCPGs.

I - HP's Role in Evolved Oscillators

In order to understand how this HP mechanism impacts behavioral performance, we have chosen to implement it in CTRNNs performing a simple task: central pattern generation at a target frequency. This task is of particular interest due to its biological significance, especially in connection with experimental studies of homeostatic plasticity

in various central pattern generating circuits (Northcutt and Schulz, 2019). Additionally, it is well-characterized in artificial dynamic networks; much is known, for instance, about the prevalence of oscillating circuits in CTRNN parameter space (Beer, 2006).

Our first goal was to evolve networks with active homeostatic regulation to succeed at this task. To reduce the impact of ceiling and floor effects, we set our target oscillatory frequency at a reasonably quick, but not maximal, 0.1 Hz (1 cycle per 10 arbitrary time units - hereafter called seconds) and performed 50 evolutionary runs with populations of 50 lasting 50 generations each. More specifically, we employed a microbial evolutionary algorithm with an elitism fraction of .1, and the rest of the population filled out every generation by mutating the top individuals from a normal distribution with variance .1 at every genomic locus without crossover (Harvey, 2011). Our fitness function took the form:

$$1 - (1/T^2)(x - T)^2 \tag{5}$$

Here, x is the measured frequency of oscillation, and T is the target frequency. Maximum fitness occurs at a frequency of T (in this case, 0.1 Hz), with a smooth decline to zero fitness at a frequency of 0 Hz (no oscillation), as well as at $2T$ (in this case, 0.2 Hz). We measured oscillatory frequency by passing a transient of 500 seconds, defining a sphere of radius 0.05 around the system's position in neural state space, counting how many seconds the system took to leave and then return to this sphere, and taking the reciprocal to yield frequency in cycles/second (Hz). Circuits were integrated using the Euler method with a timestep of .01. Finally, to ensure comparability of results, all runs held neural time-constants (τ_i) equal to 1 and weights and biases were confined within $[-16, 16]$.

The best individual in all evolutionary runs reached a fitness $\geq$0.999996, meaning all evolved frequencies fell within 0.002 Hz of the target value. Our next goal was to examine the role of HP in successful circuits. We turned HP "off" (froze the neural parameters) to observe if there was any change in frequency that might point towards an answer. To our surprise, in 7 of the 50 circuits we observed, this stopped oscillation completely (Figure 1A). This indicates that, at least occasionally, HP plays a major constitutive role in the central pattern generation at a target frequency. We will call this phenomenon *HP-enabled* oscillation.

In addition to the neural states, we tracked the values of weights and biases during simulation of each circuit as they changed according to equations 2 and 3. Intuitions put forth about biological homeostatic plasticity suggest that its main function is to configure the parameters of a circuit such that it is able to oscillate under its own power (Golowasch et al., 1999). As such, we expected parameters to show some initial amount of change as HP moves the circuit through parameter space, avoiding parameter configurations that lead to saturation and seeking those where limit cycles exist. Then once neurons start oscillating, we expected them to stabilize. Some parameter fluctuations may still occur if the adopted limit cycle forces neural output values outside the target range, but as artifacts, it seems these should be minimal. Indeed, this appears to be the case in the majority of successful circuits (Figure 1B). However, we found that parameter values tend to oscillate more appreciably in circuits where HP is necessary for oscillation, and more importantly that these parameter oscillations are crucial for generating neural oscillations.

These investigations highlight an important feature of homeostatic circuits that has not been adequately characterized. Namely, a circuit employing HP no longer has the same dimension as one of the same size with static parameters; under the influence of HP, the weights and biases become states of the system. As such, a homeostatic circuit of size n has not n dimensions, but $n^2 + 2n$ dimensions (n neural states and n^2+n changing "parameters"), and exhibit limit cycles which traverse these dimensions. Again, note that parameter oscillations alone do not indicate whether HP plays an enabling (or constitutive) role in oscillation. Some other criteria, possibly related to the range over which neural parameters oscillate, might be a more reliable indicator. To examine this distinction in more depth, we decided to reduce the dimensionality of the system to the extent that we could visualize its trajectories in this clarified state space.

II - Detailed Analysis of a Simplified System

Our next goal was to study the phenomenon of HP-enabled oscillation on a smaller, more tractable scale. Reducing the dimensionality of the system should preserve the range of possibilities regarding HP's role in central pattern generation, while allowing visualization of trajectories in state space to build intuitions.

We will be examining circuits of two fully-connected neurons and restricting the influence of HP to only one neural parameter: the bias of neuron one (θ_1). As such, the relevant system of ODE's is now defined as follows:

$$\begin{aligned}
\tau_1 \dot{y_1} &= -y_1 + w_{11}\sigma(y_1 + \theta_1) + w_{21}\sigma(y_2 + \theta_2) \\
\tau_2 \dot{y_2} &= -y_2 + w_{12}\sigma(y_1 + \theta_1) + w_{22}\sigma(y_2 + \theta_2) \\
\tau_\theta \dot{\theta_1} &= \rho_1
\end{aligned}$$

Broadly, our approach begins with initializing a homeostatic circuit and allowing it to settle into an attractor; we focus on limit cycles. Over the course of a run with non-static dynamics, θ_1 is expected to take on a range of values under homeostatic control. We will then contrast the behavior of the full homeostatic CTRNN with what is expected of non-homeostatic circuits where θ_1 is fixed at various points in that range of values (i.e. perform bifurcation analysis with respect to θ_1). This may explain how oscillations arise in the full homeostatic system even when they would not exist

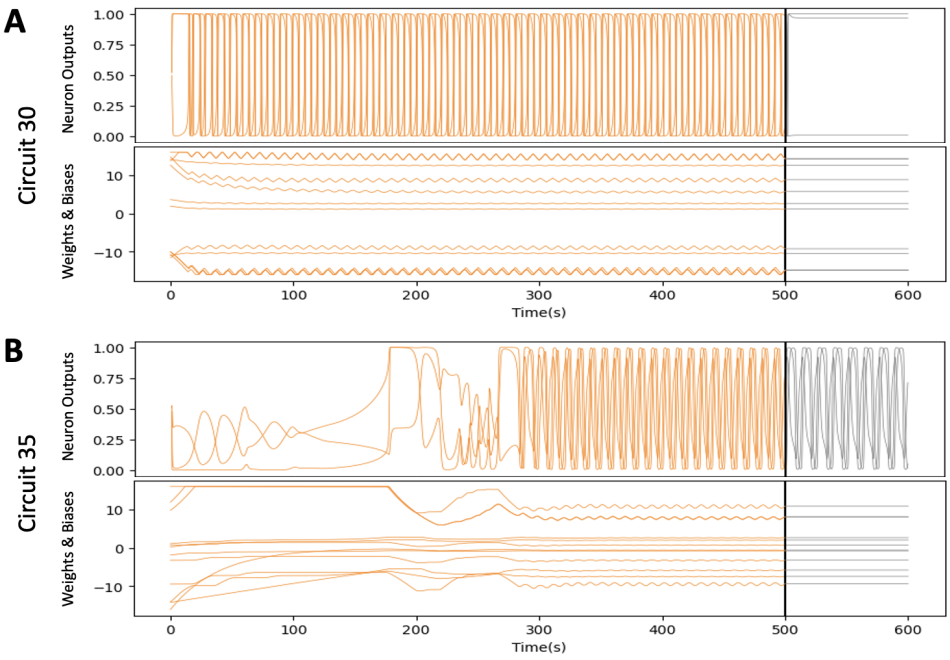

Figure 1: ***HP is necessary for some kinds of oscillatory behavior.*** **A)** Circuit evolved to attain an oscillation frequency of .1 Hz with HP on (left), which ceases to oscillate when HP is turned off (right). **B)** Another evolved circuit, with oscillation which persists after parameters are frozen. Notice that parameters themselves (weights and biases) oscillate in both cases. Vertical black line indicates the when HP has been turned off.

with static parameters, and how this relates to the observed degree of parameter oscillation.

We first randomly generated initial parameters for 1000 homeostatic circuits of size $n = 2$ and tested them for oscillation. Then, we allowed HP to act on θ_1 for 500 seconds and tested for oscillation with HP on. Finally, we froze the value of θ_1 and tested once more. Weight and bias values were initialized in the range $[-16, 16]$ and neural time constants within $[.5, 10]$. We follow the procedure of Beer (2006) to classify circuits as oscillatory or static, first summing the total amount of change in each neuron's output over a test period of 50 seconds. If this sum exceeds 0.05 for either neuron, we take this as an indication of a non-static equilibrium and label it "oscillatory". We repeated this procedure three times for each generated circuit, each time re-initializing the neural states at random values in $[-16, 16]$. Of the 1000 circuits we generated, 635 of them always exhibited oscillations while HP was on (no matter the initial condition). When HP was subsequently turned off, 564 of these always stopped oscillating. In other words, a large proportion of the random oscillatory circuits depended on the dynamics of HP to oscillate. 66 of them continued to oscillate even after HP was turned off, all but one of which had not been oscillating prior to the action of HP. That is, oscillations in those circuits were induced by HP but did not continue to require it. This leaves 5 circuits whose fate differed between initial conditions; in some trials, turning HP off stopped oscillations and in others it continued.

We have thus isolated three qualitatively different scenarios with respect to HP's role in central pattern generation. The first type of oscillation, which we will call HP-independent, is one which persists once HP is turned off, across all initial conditions. The second, which we have been calling HP-enabled oscillation, depends on HP and never continues once it is deactivated. The third mode is that in which turning HP off only sometimes interrupts oscillations. For reasons which will be made clear, we will call this partially HP-enabled oscillation. Now, we will choose representative circuits from each group and analyze the limit cycles they exhibit in the manner described previously.

Figure 2A depicts the bifurcation diagram of an HP-independent oscillator. In the non-plastic version of this circuit, as θ_1 varies from -15 to -2 the system passes through two SNIC bifurcations which give rise to and then destroy a limit cycle in neural output-space (blue). The orange trajectory shows one way the homeostatic version of this circuit might navigate this space. Being initialized with a bias value of -5, the neural states make their way towards the only stable equilibrium point available. At this equilibrium point, neuron 1's output is too high, prompting the HP mechanism to reduce the value of θ_1. Eventually, it is reduced far enough that a limit cycle is born, which the neural states begin to follow. Notice that, along one side of this limit cycle, the output of neuron 1 actually falls below the boundary

of HP's target activity range, prompting a slight increase in the value of θ_1, which is then directly offset by a decrease when it exceeds the upper boundary. This results in small-magnitude oscillations in the θ_1 dimension, which continue indefinitely. However, throughout the whole length of this homeostatic limit cycle, θ_1 never crosses into a region of CTRNN parameter space without a limit cycle. As such, no matter the point at which HP may turn off, oscillations would persist in this circuit.

The bifurcation diagram depicted in Figure 2B is an example of an HP-enabled circuit. Here we see that, as θ_1 increases, fold bifurcations first introduce a new stable fixed point and then destroy the original one. As such, a homeostatic circuit initialized with $\theta_1 = -1.6$ (orange trajectory) first approaches the lower equilibrium point. Once there, HP starts to increase θ_1 because the output of neuron 1 is too low. Eventually, this equilibrium point ceases to exist, so the neural states fall into the upper equilibrium branch. The value of neuron 1 at this equilibrium point is too high, so θ_1 is decreased until that equilibrium disappears and the cycle repeats, generating oscillations in both θ_1 and the neural states. Of course, if HP is turned off at any point in this limit cycle, oscillations will stop.

Finally, we can use this framework to account for the third scenario, wherein oscillation only sometimes persists after HP is off (Figure 2C). In this case, the orange example trajectory begins with $\theta_1 = -3.5$. At the stable equilibrium point neuron 1's output is too low, so θ_1 increases until a limit cycle is born, which the neural states follow. This limit cycle takes neuron 1's output above the target range, at which point the system assumes a trajectory which decreases θ_1 yet again. As such, the homeostatic system adopts a limit cycle that is mostly enabled by changes in θ_1. However, it does lead the system through an area of parameter space where HP-independent oscillations exist. If HP happens to be turned off during that section of the limit cycle, oscillations will persist. Therefore, we call this type of oscillator *partially* HP-enabled.

Keeping in mind our goal of studying the role of HP acting concurrently with behavior (that is, not "turned off"), what do these analyses have to offer? For one, they point to some defining characteristics that might help to distinguish these three scenarios *without* the need to actually manipulate HP. Abstract bar representations below each of the three bifurcation diagrams serve to highlight the range of θ_1 in which limit cycles exist in the non-homeostatic system (blue) and the range of θ_1 traversed by the homeostatic system (orange). We have already seen how their degree of overlap affects the result of turning HP off. However, it also highlights the fact that limit cycles which are dependent on HP tend to encompass a wider range of bias values. Thus, as suggested in Section I, the range of values traversed by the neural parameters during oscillation may provide clues as to whether that oscillation is HP-enabled or not. Of course, we now understand that this is ultimately relative to the range of parameter values in which oscillations exist without HP.

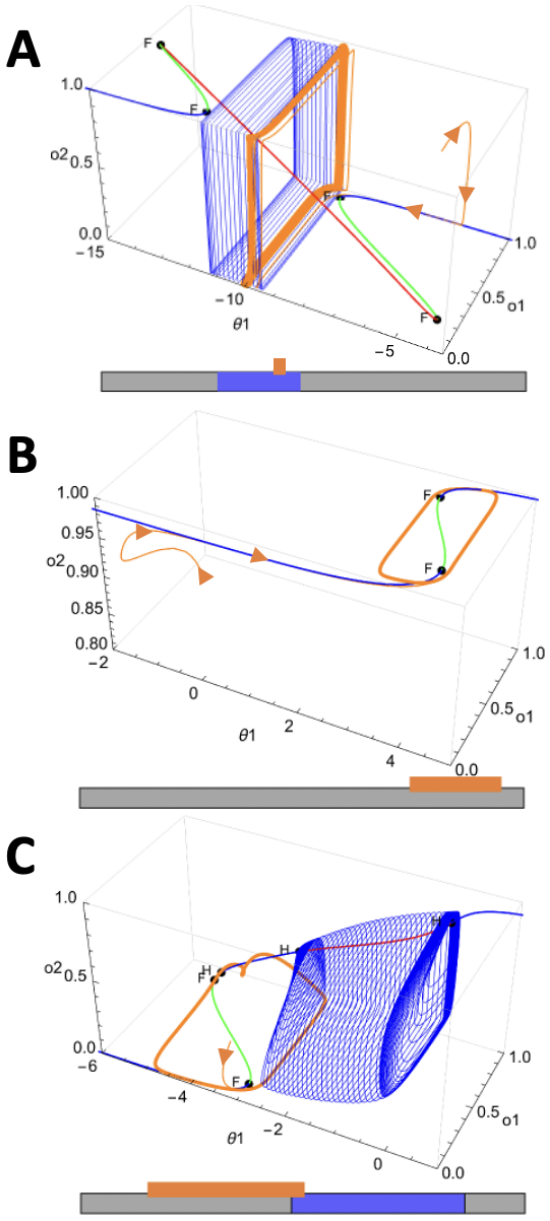

Figure 2: ***Three modes of HP involvement in oscillation.*** **A)** "HP-independent" oscillations do not rely on HP at any point in the homeostatic limit cycle. **B)** "HP-enabled" oscillations depend on HP for the whole duration of the limit cycle. **C)** "Partially HP-enabled" oscillations depend on HP through portions of the limit cycle, but it also passes through a region of parameter space where oscillations exist on their own. Accompanying colored bars are of approximate scale to visualize the range of θ_1 in which limit cycles exist in the static system (blue) and the range of θ_1 traversed by the limit cycle of the homeostatic system (orange).

III - Parameter Space Sampling

Thus far, we have furnished the space of possibilities with three qualitatively distinct modes of homeostatic involvement in oscillation. Two of them (HP-enabled and partially HP-enabled) require that HP remain active during behavioral performance. This is a departure from the typical conception of HP, which holds that its main role is to push circuits into regions of parameter space where limit cycles involving neural states exist, and then it becomes functionally irrelevant. This possibility is approximately represented in our framework by HP-independent oscillators, which may have been initialized as non-oscillators and then guided into oscillatory regions of parameter space where they remain. But relatively how likely are each of these scenarios to arise in a randomly generated homeostatic network? Our investigations from Section II suggest that purely HP-enabled oscillation may be very common. Indeed, over half of those randomly generated simple circuits exhibited HP-enabled oscillations, compared to $\sim$6% which were HP-independent. But how does this generalize to the full HP mechanism implemented on circuits of various sizes? We hope to answer this question by conducting thorough parameter space sampling.

For circuit sizes between $n = 1$ and $n = 20$, we first randomly generated a sample of 10^4 non-homeostatic CTRNNs with weight and bias values initialized in the range $[-16, 16]$ and neural τ_i's in the range $[.5, 10]$. Using an Euler integration step size of 0.1, we allowed transients to pass for 5000 steps before checking for oscillation, as described previously. This procedure was repeated 10 times for each generated circuit, each time initialized from a different point in neural state space. If oscillatory activity was detected for any one of these repetitions, the circuit itself was classified as oscillatory. This constitutes the "no-HP" condition.

The procedure was repeated for a sample of homeostatic CTRNNs which passed a transient of 5000 steps and were tested for oscillation while HP remained active. We expect this group to include instances of HP-enabled oscillation, in addition to partially HP-enabled and HP-independent oscillators. This was the "HP-on" condition. Finally, we generated a sample of circuits to which HP was applied over the course of 5000 time steps and then turned off. Oscillation was checked after passing a transient of 5000 time steps following shutoff ("HP-off" condition). In order to ensure a fair comparison of oscillatory probability with non-homeostatic circuits, HP was prevented in all cases from pushing weights and biases outside the $[-16, 16]$ range.

In Figure 3, we plot the proportion of oscillators in the no-HP (blue), HP-off (green), and HP-on (orange) samples. Crucially, the probability that a circuit with active HP will oscillate is extremely high across circuit sizes. If the main effect of HP on oscillatory dynamics could be accounted for by HP-independent oscillations (i.e. simply pushing the circuit into an oscillatory region), then continued oscillation in the HP-off condition should be just as common as in the HP-on condition. We see that this is not the case (orange vs. green lines), indicating that HP-enabled oscillations are very common in this system. Still, the temporary action of HP has some influence, greatly increasing the probability that a circuit oscillates as compared to random non-homeostatic circuits (green vs. blue lines).

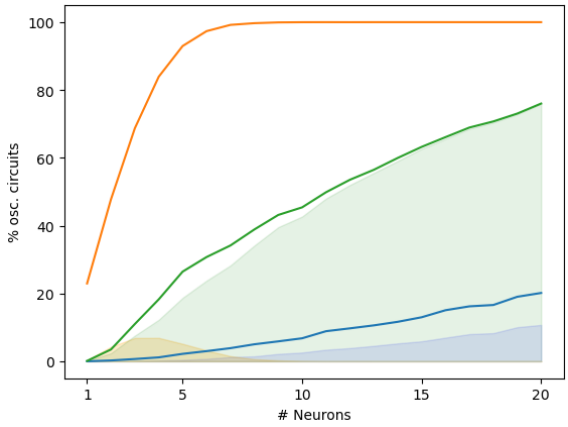

Figure 3: ***Partially and fully HP-enabled oscillations are common across circuit sizes.*** **Blue:** A sample of 10^4 randomly generated non-homeostatic circuits of various sizes had few oscillators, a consistent proportion of which sometimes fail to reach their limit cycle (blue area). **Green:** Circuits where HP was on briefly then shut off had an intermediate probability of oscillating, virtually all of these continuing oscillators being unreliable (green area). **Orange:** Circuits tested with HP on were very likely to oscillate and almost never contingent on initial condition (orange area).

As previously mentioned, the dimensionality of a homeostatic network is greater than that of a non-homeostatic network with the same number of nodes. In addition to its n changing neural states, it has $n^2 + n$ changing "parameters". Would HP-on and no-HP circuits of equal dimension have comparable oscillation probabilities, or is this phenomenon attributable to the action of HP specifically? We can see that the former is unlikely to be the case by comparing, for instance, HP-on circuits of size $n = 2$ (48% oscillating) to no-HP circuits of size $n^2 + 2n = 8$ (5% oscillating). Therefore, continued homeostatic parameter regulation, not just increased dimensionality, is responsible for this effect.

Note it is possible in this setup that the proportion oscillators which persist after HP is off (green) reflect a mixture of HP-independent oscillation and partially HP-enabled oscillation. We sought to differentiate these two by recording the proportion of circuits in each sample for which classification as an oscillator varied between initial conditions: "sporadic" oscillators. That is, if there was at least one trial featuring oscillations, the circuit was classified as an oscillator, but if there was also at least one trial that did not feature oscillations, the circuit was also classified as a sporadic oscillator.

The proportion of sporadic oscillators under each condition is represented by the shaded areas in Figure 3.

As indicated by the size of the green-shaded area of Figure 3, virtually none of the circuits which sometimes kept oscillating after HP turned off did so consistently. Continued oscillation was almost always unreliable, especially for larger circuit sizes. We take this as evidence that even circuits which persist in oscillation after HP is turned off do so primarily because HP happened to have been turned off in a favorable portion of a homeostatically-enabled limit cycle, not because the limit cycle was HP-independent. In principle, this proportion also captures cases where the homeostatic system occasionally fails to oscillate, leaving the circuit in a stable equilibrium. However, as conveyed by the size of the orange-shaded area, that situation is not very common. It is also likely the case that there are many possible limit cycles that a homeostatic system could adopt, some being HP-independent while others are not. Teasing apart these hypotheses is left to future studies.

IV - Systematically Varying HP's Timescale

We have seen that the timescale chosen for HP so far ($\tau_\theta = 20, \tau_w = 40$) allows it to participate extensively in central pattern generation. So much so, in fact, that neural state oscillations are routinely modified in frequency by HP (Figure 2A&B orange limit cycles vs blue limit cycles) and commonly completely depend on HP for their realization (Figures 2C&3). Would this still be the case if HP operated on a much slower timescale relative to the neural states, or is there a certain degree of timescale separation at which we would be justified in saying that HP-enabled oscillations are insignificant compared to those that would exist independently? To investigate this question, we systematically varied the degree of timescale separation in the model between the rate of change of neural states and neural parameters and observed its effect on HP's role in central pattern generation.

For simplicity in these experiments, we ensured that the time constant for the changing biases (τ_θ) was equal to that for the changing weights (τ_w). With all neural time constants $\tau_i = 1$, the ratio of HP time constants to neural time constants is thus equal to the value of $\tau_\theta = \tau_w$. Note also that we have adjusted our method of detecting oscillation frequency, having realized that the system is not autonomous with respect to the neural states alone. We now define a sphere of radius 0.075 around the circuit's initial point in $n^2 + 2n$ dimensional space and record how long it takes for its trajectory to leave and return to that sphere.

First, for each integer value of $\tau_\theta = \tau_w$ from $[1, 100]$, we evolved 25 circuits with HP (as in Section I) for oscillation at a target frequency of .1. Ten attempts were made to reach a fitness of .999996 (corresponding to a frequency within .002 Hz of the target) and data from trials where this wasn't achieved were discarded. For evolutionary runs that did reach the fitness threshold, we then measured the oscillation

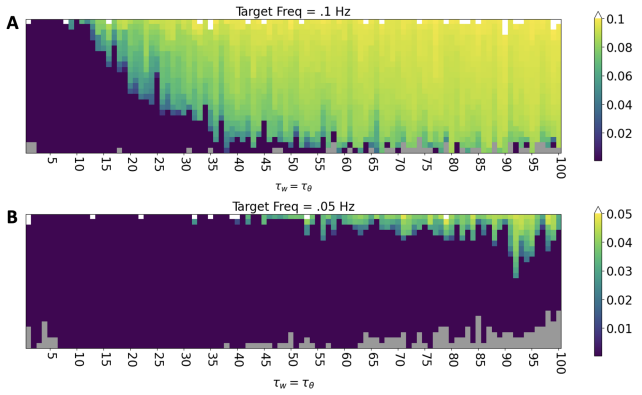

Figure 4: ***HP is more likely to modulate or enable slower oscillations, especially when its timescale is closer to neural activity.*** **A)** Osc. frequency of circuits ($n = 3$) which evolved with HP on to match a target freq. of .1 Hz, then had HP turned off. When the timescale of HP is close to that of the neural parameters (left), many circuits exhibit reduced or zero frequency without HP. This effect lessens as HP gets slower relative to neurons (right). **B)** Circuits evolved to match slower osc. frequency of .05. HP was likely to have enabled oscillation in more cases, especially when operating on timescales closer to that of neurons (left). Evolutions where circuits failed to reach a fitness of .999996 represented by grey pixels.

frequency of the best individual *without* HP. This reveals the extent to which HP had been contributing to the achievement of the target frequency—ranging from no involvement, to moderate frequency modulation, to HP-enabled oscillation.

Resulting frequencies are shown in Figure 4A, with each trial represented by a colored pixel. At low degrees of timescale separation when parameters are changing nearly as fast as neural states (left), circuits frequently stop oscillating without HP. That is, evolution is likely to have found an HP-enabled oscillation to match the target frequency. As HP gets slower relative to the neural states, this becomes less and less likely. At intermediate values, HP is often still involved, appreciably boosting the frequency of HP-independent oscillations. Eventually, though, even this becomes uncommon, with most all circuits continuing to oscillate at about the same frequency (.1) with or without HP. In other words when HP is very slow (right), it appears that only oscillations which rely on the neural states (HP-independent) can effectively meet the frequency demands. As such, evolution has fewer options for creating a suitable oscillator, and more failures are encountered (grey pixels).

Given that the target frequency seems to have had some bearing on the results of this experiment, we repeated the procedure with a target half as fast (0.05 Hz). Figure 4B depicts the results, with a color map scaled to this new tar-

get frequency. In this case, it was significantly more likely that oscillations were HP-enabled (cease once HP is off). It appears that HP mechanisms with timescales which were previously too slow to enable oscillation (middle) are now likely to do so. Moreover, evolution seems to take full advantage of this functionality. It may even be the case that HP-independent oscillations are too fast to use; there are a significant number of evolutionary failures when HP's timescale is close to that of the neural states, as well as when HP is extremely slow (potentially too slow for HP-enabled oscillations to match .05 Hz). Overall, this suggests that the frequency of HP-enabled oscillations depends on the timescale of HP, and they are more likely to occur when HP is operating close to the timescale of behavior. However, they can occur at relatively large degrees of separation (i.e. 1:100 ratio, Fig.4B); this depends on the target frequency. Finally, even if oscillations are not fully HP-enabled, their frequency may be modulated up or down by HP.

Discussion

Through these analyses, we have begun to characterize a kind of oscillation exhibited by homeostatic circuits which fully relies on the dynamic adjustment of circuit "parameters". This HP-enabled oscillation cannot be sustained without HP and highlights the fact that homeostatic circuits are fundamentally different, higher-dimensional systems than non-homeostatic ones. It is misleading to consider HP as acting *upon* a base circuit, simply pushing it into favorable regions of parameter space and then sitting idle; doing so neglects the possibility of emergent dynamics like this.

Importantly, just because HP-enabled oscillators rely on HP for their dynamics does not inherently mean they are less suitable as a behavioral substrate. In fact, when considering the task of pure central pattern generation, they have the advantage of being extraordinarily common and easy to generate. They are also better able to deal with parameter perturbations which would disrupt non-plastic oscillators (Williams, 2004). However, in the context of the more complex tasks studied by Williams (2004, 2005), HP-enabled oscillations disrupted behavioral fitness. As our analysis elucidates, systems employing HP are rarely ever found at equilibrium points and by definition these equilibria never involve neural saturation. Equilibria and saturation, however, may be crucial to the performance of these tasks. This, in combination with other factors, could be the reason why CTRNNs employing HP during performance are less fit phototaxers, shape discriminators, and ball-catchers.

Future Directions

There are several ways this model could be improved to simultaneously boost performance and provide insight into biological HP. Ultimately, the ideal HP mechanism will prevent a circuit from adopting unfavorable activity profiles while allowing activity profiles suited to its behavioral goals. We have seen this is easier said than done. Adjustment of the target output range, or the addition of sliding window averaging to detect activity may make HP more permissive and useful. Similarly, one may consider applying HP differentially throughout the circuit.

Another important avenue for future inquiry is whether homeostatic plasticity can drive oscillations in real neural circuits. As mentioned previously, the changes in synaptic and intrinsic excitability that have been attributed to HP generally take place over the course of minutes to hours, not seconds as depicted here to follow existing conventions. However, the time units used in this analysis are completely arbitrary. There are certainly rhythmic behaviors which take place on these slower timescales (take circadian rhythms, for example) and which may rely on HP in the manner described. The most important point suggested by these analyses is that, so long as there is some degree of overlap between the timescale of HP and the timescale of behavior, HP is likely to play not only a passive, but a constitutive role in central pattern generation. Moreover, we have seen that the timescales of these respective processes need not be particularly close for this to occur. This is especially true if one considers that HP may appreciably modulate oscillation frequency, even if it does not fully enable it. Taken with the fact that organisms rely on rhythmic behaviors across a variety of timescales, it is plausible (if not probable) that some of these oscillations might depend on processes that operate homeostatically.

Ultimately, investigating these kinds of questions will require a dialogue between models and experiment. Should we expect, for example, to detect rhythmic changes in synaptic strength phase-locked to neuronal bursting patterns just as we see oscillating CTRNN weights? Additionally, we have just shown that disrupting HP can provide insight into its function; it may be illuminating to do so in the lab. Furthermore, models like this one can suggest feature differences between HP-enabled and HP-independent oscillations which may be used to identify them in real systems. We have suggested, for instance, that HP-enabled oscillations are slower than HP-independent ones, and accompanied by more parameter fluctuation. More biophysically realistic models of HP may be a useful intermediate step toward testing these theories. Overall, this modeling framework presents many opportunities for dialogue between theory and experiment, as well as the general application of dynamical systems theory to tackle biological questions.

Acknowledgements

We would like to thank Connor McSchaffrey, Eden Forbes, Zachary Laborde, Gabriel Severino, Andrew Claros, Maria Pope, and Jason Yoder for their insights regarding this project and its presentation. In addition, we thank the anonymous reviewers for their helpful feedback. This work was supported in part by NSF grants 1845322 and 1735095.

References

Abbott, L. F. and LeMasson, G. (1993). Analysis of Neuron Models with Dynamically Regulated Conductances. *Neural Computation*, 5(6):823–842. ZSCC: 0000093.

Beer, R. D. (2006). Parameter Space Structure of Continuous-Time Recurrent Neural Networks. *Neural Computation*, 18(12):3009–3051. ZSCC: 0000114.

Davis, G. W. (2006). Homeostatic Control of Neural Activity: From Phenomenology to Molecular Design. *Annual Review of Neuroscience*, 29(1):307–323. _eprint: https://doi.org/10.1146/annurev.neuro.28.061604.135751.

Di Paolo, E. (2002). Evolving Robust Robots Using Homeostatic Oscillators. *University of Sussex*. ZSCC: 0000018.

Di Paolo, E. A. (2000). Homeostatic Adaptation to Inversion of the Visual Field and Other Sensorimotor Disruptions.

Golowasch, J., Casey, M., Abbott, L. F., and Marder, E. (1999). Network Stability from Activity-Dependent Regulation of Neuronal Conductances. *Neural Computation*, 11(5):1079–1096. ZSCC: 0000187 Conference Name: Neural Computation.

Günay, C. and Prinz, A. A. (2010). Model Calcium Sensors for Network Homeostasis: Sensor and Readout Parameter Analysis from a Database of Model Neuronal Networks. *Journal of Neuroscience*, 30(5):1686–1698.

Harvey, I. (2011). The Microbial Genetic Algorithm. In Kampis, G., Karsai, I., and Szathmáry, E., editors, *Advances in Artificial Life. Darwin Meets von Neumann*, Lecture Notes in Computer Science, pages 126–133, Berlin, Heidelberg. Springer.

He, L. S., Rue, M. C., Morozova, E. O., Powell, D. J., James, E. J., Kar, M., and Marder, E. (2020). Rapid adaptation to elevated extracellular potassium in the pyloric circuit of the crab, Cancer borealis. *Journal of Neurophysiology*, 123(5):2075–2089. Publisher: American Physiological Society.

Lane, B. J., Samarth, P., Ransdell, J. L., Nair, S. S., and Schulz, D. J. (2016). Synergistic plasticity of intrinsic conductance and electrical coupling restores synchrony in an intact motor network. *eLife*, 5:e16879.

Liu, Z., Golowasch, J., Marder, E., and Abbott, L. F. (1998). A Model Neuron with Activity-Dependent Conductances Regulated by Multiple Calcium Sensors. *The Journal of Neuroscience*, 18(7):2309–2320. ZSCC: 0000265.

Mathayomchan, B. and Beer, R. D. (2002). Center-Crossing Recurrent Neural Networks for the Evolution of Rhythmic Behavior. *Neural Computation*, 14(9):2043–2051.

Northcutt, A. J. and Schulz, D. J. (2019). Molecular mechanisms of homeostatic plasticity in central pattern generator networks. *Developmental Neurobiology*, 80(1-2):58–69. _eprint: https://onlinelibrary.wiley.com/doi/pdf/10.1002/dneu.22727.

Olypher, A. V. and Prinz, A. A. (2010). Geometry and dynamics of activity-dependent homeostatic regulation in neurons. *Journal of Computational Neuroscience*, 28(3):361–374. ZSCC: 0000036.

O'Leary, T., Williams, A. H., Franci, A., and Marder, E. (2014). Cell Types, Network Homeostasis, and Pathological Compensation from a Biologically Plausible Ion Channel Expression Model. *Neuron*, 82(4):809–821.

Schulz, D. J. and Lane, B. J. (2017). Homeostatic plasticity of excitability in crustacean central pattern generator networks. *Current Opinion in Neurobiology*, 43:7–14.

Thoby-Brisson, M. and Simmers, J. (2000). Transition to Endogenous Bursting After Long-Term Decentralization Requires De Novo Transcription in a Critical Time Window. *Journal of Neurophysiology*, 84(1):596–599. Publisher: American Physiological Society.

Turrigiano, G. (2012). Homeostatic synaptic plasticity: local and global mechanisms for stabilizing neuronal function. *Cold Spring Harbor perspectives in biology*, 4(1). ZSCC: 0000829.

Turrigiano, G., Abbott, L. F., and Marder, E. (1994). Activity-dependent changes in the intrinsic properties of cultured neurons. *Science*, 264(5161):974–977. ZSCC: 0000553 Publisher: American Association for the Advancement of Science.

Turrigiano, G. G. and Nelson, S. B. (2004). Homeostatic plasticity in the developing nervous system. *Nature Reviews Neuroscience*, 5(2):97–107. ZSCC: 0002437.

Watt, A. and Desai, N. (2010). Homeostatic plasticity and STDP: keeping a neuron's cool in a fluctuating world. *Frontiers in Synaptic Neuroscience*, 2.

Williams, H. (2004). Homeostatic Plasticity in Recurrent Neural Networks. In *From animals to animats 8: Proceedings of the Eighth International Conference on the Simulation of Adaptive Behavior*, pages 344–353. MIT Press, Cambridge, MA.

Williams, H. (2005). Homeostatic plasticity improves continuous-time recurrent neural networks as a behavioural substrate. *Proceedings of the International Symposium on Adaptive Motion in Animals and Machines, AMAM2005*. ZSCC: 0000009.

Williams, H. (2006). *Homeostatic adaptive networks*. Doctoral Dissertation, University of Leeds, UK. ZSCC: 0000023.

Williams, H. and Noble, J. (2007). Homeostatic plasticity improves signal propagation in continuous-time recurrent neural networks. *Bio Systems*, 87(2-3):252–259. ZSCC: 0000037.